Food Chemistry: X 19 (2023) 100757

Contents lists available at ScienceDirect

Food Chemistry: X

journal homepage: www.sciencedirect.com/journal/food-chemistry-x

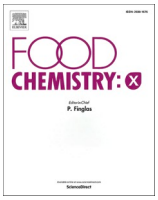

Inherent molecular characteristics and effect of garlic polysaccharides on dough micro- and mesoscopic properties

Qian Li [a,b,c], Jiaming Liu [a,d], Huiqi Wan [a], Min Zhang [a,b,c,*]

[a] Tianjin Agricultural University, Tianjin 300392, PR China
[b] China-Russia Agricultural Processing Joint Laboratory, Tianjin Agricultural University, Tianjin 300392, PR China
[c] State Key Laboratory of Nutrition and Safety, Tianjin University of Science & Technology, Tianjin 300457, PR China
[d] Tianjin Guangyuan Livestock and Poultry Breeding CO., LTD, Tianjin 301800, PR China

ARTICLE INFO

Keywords:
Garlic supernatant polysaccharides
Non-starch polysaccharides
Dough properties

Chemical compounds:
Trifluoroacetic acid (PubChem CID: 6422)
Sodium borohydride (PubChem CID: 4311764)
Acetic anhydride (PubChem CID: 7918)
Pyridine (PubChem CID: 1049)
Potassium bromide (PubChem CID: 253877)

ABSTRACT

Directional control of the process of doughs with nutrition fortification is challenging. Thus, this study aimed to develop non-starch polysaccharides that can modify the quality of flour products. Polysaccharides were extracted from three different garlic cultivars, evaluated for physicochemical properties and used to enrich doughs for microstructure and mesoscopic characteristics analysis. We assessed the moisture distribution, texture characteristics, thermodynamic properties, dynamic viscoelastic properties, protein structure, microstructure and molecular interaction of the doughs and demonstrated a relatively high molecular weight, lower steric hindrance of molecular chains and higher cross-linking ability with the dough network in the supernatant polysaccharide from Yunnan single-clove-garlic (SGSOS) fraction. These features of SGSOS fraction improved the rheological, thermodynamic, texture characteristics, and water distribution of doughs. These findings provide information on the use of garlic polysaccharides during the processing and manufacturing of foods to enhance their processing adaptability and qualities.

1. Introduction

The increase in the global population and living standards has resulted in high demand for highly safe food products with higher nutrition value, better flavour and good texture quality. Flour products are staple foods for several people worldwide and constitute a high proportion of daily diets because of their high nutritional value and several health benefits. The Chinese Food Science and Technology Society statistics indicate that the market share of flour-containing foods, such as steamed bread and noodles, is more than 600 billion Yuan. However, the relationships between the dough components and their effects on the quality of flour products have not been fully elucidated (Bozkurt, Gorguc, Gencda, Elmas, Koc & Yilmaz, 2023). Therefore it is imperative to improve the techniques used in developing flour products and formulate strategies to control the status of intermediate products and quality of final products to achieve transformation of resource advantages to economic advantages and solve food shortages.

The physicochemical properties of doughs during the processing largely depend on the micro- and mesoscopic properties, such as the protein secondary structure, rheological behaviour, thermodynamic properties and the cross-linking effects between the components in the dough (Sun, Wu, Koksel, Xie & Fang, 2023). However, it is challenging to meet the development requirements of modern nutritious and healthy food to enhance the processing adaptability of doughs by focusing on the physicochemical or nutritional characteristics of a single component in an isolated way due to the polyphase and multicomponent system of the dough system (Thanushree, Sudha, Martin, Vanitha & Kasar, 2022).

Previous findings indicate that adding non-starch polysaccharides to dough improves the nutritional properties of flour products, resulting in different effects on their structure and physicochemical properties (Falsafi, et al., 2022). Adding polysaccharide fractions to dough can also supplement the non-starch polysaccharides required by our bodies and improve the texture, flavour and other qualities of flour products (Renzetti & van der Sman, 2022). These effects are due to the impacts of non-starch polysaccharides on the formation and continuity of the gluten network by interacting with gluten protein (Li, et al., 2023). This also changes the strength and density of the gluten network number and uniformity of internal pores. The interaction mechanism between the multi-component dough systems is probably different from that between single components (Wang et al., 2022). Therefore, it is imperative to

* Corresponding author at: China-Russia Agricultural Processing Joint Laboratory, Tianjin Agricultural University, Tianjin 300392, PR China.
E-mail address: zhangmin@tjau.edu.cn (M. Zhang).

https://doi.org/10.1016/j.fochx.2023.100757
Received 13 April 2023; Received in revised form 31 May 2023; Accepted 15 June 2023
Available online 20 June 2023

systematically explore the cross-link effects between polysaccharides and other components in the dough. Furthermore, the molecular mechanism in the multi-component system should be analysed to provide a basis for formulating effective strategies to enhance the adjustability and quality of flour products under processing or storage conditions.

Garlic has valuable non-starch polysaccharide compounds, mainly fructose, glucose and galactose, with several other functional benefits including treating various health conditions due to their numerous physiological effects (Qiu, Qiao, Zhang, Sun-Waterhouse & Zheng, 2022). Their fractions are used as prebiotics to control the gut microflora and their metabolites can significantly reduce the amount of intestinal non-beneficial bacteria and the risk of metabolic disorders, such as alcoholic liver injury and cardiovascular diseases (Zhang, Jin, Wang, Zhang, Shah & Wei, 2022). Foods fortified with garlic polysaccharides can enhance the immune system by activating multiple signalling pathways, while consuming those rich in such polysaccharides can alleviate various health conditions associated with oxidative stress mitigating the effects of hydroxyl or superoxide anion radicals and serum or liver lipids in the body, due to their scavenging functions.

Therefore, doughs can be fortified with garlic polysaccharide fractions to produce high-fibre and low-calorie food products with high fiber and low calories. The properties of garlic polysaccharides-enriched dough significantly depend on the contents of the polysaccharide fractions and cross-linking effects between the components induced by the polysaccharides fractions in the dough, predominantly gluten protein. For example, the addition of excessive garlic polysaccharide fractions can reduce the appearance, flavour and texture of flour products, which is a key challenge when manufacturing non-starch polysaccharides-enriched foods (Wang et al., 2022). As a result, it is imperative to explore the complex cross-linking effects of ingredients in garlic polysaccharide-based food systems and the influences of their impact on the processing, adaptability and properties of the final flour-based products. This analysis can provide insights into the development of non-starch polysaccharides-enriched foods. A few studies have explored the cross-linking effects between garlic polysaccharide fractions and other dough components and their impact on dough micro- and mesoscopic characteristics. This is partly attributed to the complexity of the matrix of food raw materials, resulting in the formation of a complex network and technical challenges in analysing the molecular feature. Supplementation of polysaccharides might also have controversial effects on the processing, adaptability and properties of doughs, which can be ascribed to the polysaccharides' architecture, such as molecular masses, steric hindrance of molecular chains, and the corresponding functions. Therefore, systematic studies on the cross-linking effects between garlic polysaccharide fractions and dough networks should be conducted to provide information on the application of garlic polysaccharide-based flour products.

In the present study, we explored the micro- and mesoscopic features of three garlic supernatant polysaccharides fractions (supernatant polysaccharide from Yunnan single-clove-garlic (SGSOS), supernatant polysaccharide from Tianjin purple-skin-garlic (PGSOS) and supernatant polysaccharide from Cangshan hybridize-garlic (HGSOS) extracted from different garlic plants in China.We also investigated, the impacts of the garlic polysaccharide fractions on the dough network by studying its rheological characteristic, moisture distribution, thermodynamic properties, textural profiles, cross-linking effects and secondary structure parameters of wheat gluten.

2. Materials and methods

2.1. Materials

We purchased Yunnan, Cangshan and Tianjin garlic varietal samples from JD.com Inc. (Beijing, China). The wheat flour purchased from Tianjin Food Group, China, comprised 74.0% of carbohydrates, 9.0% of protein, 1.5% of lipids and 14.5% of moisture.

2.2. Preparation and chemical analysis of garlic supernatant polysaccharides fractions

The garlics were peeled and polysaccharides were prepared as described previously with a few modifications (Liu, Li, Zhang, Yun & Zhai, 2022). A 100 g of peeled garlic samples were placed in a 1000 mL beaker, mixed with 500 mL ultrapure water and. incubated for 80 min at 90 °C to inactivate garlic enzymes. The filtrate was recovered by filtration at room temperature under 0.1 MPa, followed by washing with distilled water to remove the garlic pulp and then concentrated under 5.6 kPa pressure at 60 °C. The concentrated garlic supernatant polysaccharide fractions were extracted with 6 times volume of 95% ethanol (Tianjin Feng chuan Chemical Reagent Co., Ltd, Tianjin, China) for 24 h at 4 °C. The solutions were filtered and lyophilized to obtain the precipitated garlic supernatant polysaccharide samples.

Each garlic supernatant polysaccharide sample (100 mg) was redissolved in ultrapure water (1 mL) and was stored under 25 °C for 3 h. Proteins were eliminated through polyamide chromatography (Φ 6.0 cm × 30 cm in size, with a 25 cm of column bed, Sinopharm Co., Ltd.) as described previously. The polyamide column was prepared using the wet-loading method, and the column was incubated at 25 °C for 3 h. Subsequently, each garlic supernatant polysaccharide solution (5 mL) was loaded into the polyamide column within 1 min. The chromatography conditions were as follows: adsorption equilibration time, 1 h; elution speed, 3 mL/min; eluent, ultrapure water (pH 7.0); eluted volume, five times column volume then collected as one sample per 100 mL. The garlic supernatant polysaccharides were obtained from the eluents by dialysis, concentration and lyophilization.

Polysaccharides collected from Yunnan, Cangshan and Tianjin garlic samples were denoted as SGSOS, HGSOS and PGSOS, respectively. The total protein and sugar levels in the polysaccharide fractions were quantified using a Detection Kit following the manufacturer's instructions (Sigma Chemical Co. Beijing, China).

2.3. Molecular weights distribution analysis

The molecular weights of polysaccharides in garlic supernatant were determined on the 1260 Infinity II HPLC system with a 0.8 × 30 cm SB-802 HQ column (Showa Denko Scientific Instrument Co., Kyoto, Japan) as well as a differential refractive detector (RID-G1362A; Agilent Technologies Inc., CA, USA). The HPLC was calibrated using the *T*-series dextran standards provided by Sigma Chemical Co. (Beijing, China). The chromatographs were obtained and interpreted with the Agilent ChemStation system. About 1 mL of polysaccharide sample solutions (5 mg/mL) were prepared by dissolving the samples in distilled water, followed by filtration using a 0.22-μm filter membrane (Dingguo Changsheng Biotechnology Co., Ltd, Beijing, China) together with HPLC analyses. HPLC conditions included a total system volume of 20 μL column temperature of 30 ± 0.1 °C, ultrapure water as the eluent and a flow rate of 0.8 mL/min. The retention time of chromatographic peaks was recorded and analyzed relative to the retention times of standard compounds to determine the molecular weights of polysaccharides.

The weight-average molecular weight (*M*w) was calculated by dividing the total sample mass by the weight fraction of each polysaccharide (the statistical average molecular weight based on mass, which was obtained by averaging the molecular weight per unit weight) and the number-average molecular weight (*M*n) as the overall molecular number weighted average of all molecular weights of each sample. The *M*w and *M*n were computed with the measured peak areas of individual oligosaccharides (A_i) and the molecular weight of each oligosaccharide (M_i) as follows:

$$Mn = (\Sigma A_i M_i)/(\Sigma A_i); Mw = \left(\Sigma A_i M_i^2\right)/(\Sigma A_i M_i)$$

2.4. Monosaccharide components

We adopted the TM-1701 column (30 m × 0.32 mm × 0.5 μm; Tianmei Scientific Instrument Co., Ltd., Shanghai, China) to explore the monosaccharide profile in the garlic supernatant polysaccharides using the Techcomp 7900 GC system as described previously study (Liu, et al., 2022). About 10 mg of the polysaccharides were completely hydrolysed into monosaccharides by incubating with 0.5 mL trifluoroacetic acid (2 mol/L) for 5 h at 100 °C in an airtight ampoule. Excessive acid was eliminated thrice by co-distillation with 1 mL of methanol and distilled water at 50kpa and 60 °C. After monosaccharide reduction using 30 mg sodium borohydride ($NaBH_4$) for 1.5 h period at 25 °C, the excessive $NaBH_4$ was eliminated through co-distillation with 5 mL acetic acid (17.5 mol/L) at 50 kpa at 60 °C. The reduced monosaccharides were then acetylated with 0.5 mL acetic oxide-pyridine (pyridine: acetic anhydride = 1:1, v/v) and transformed to sugar alcohol acetate for 1 h at 100 °C in an airtight environment (high temperature drying oven) followed by filtering of 10 μL of the derivatives with the 0.22-μm filter membrane before Gas Chromatography (GC) analysis.

Hydrogen, N_2 and air were utilized as the fuel, carrier, and oxidant gas, with constant column flow of 30, 50, and 500 mL/min, respectively. Detector and injection temperatures were 280 and 250 °C, respectively. We typically programmed the oven temperature to increase from 130 to 180 °C at 3 °C/min, followed by a 3 min holding, an increase to 230 °C at 10 °C per 0.8 mL per minute, and an eventual rise to 280 °C at the rate of 20 °C per 0.8 mL/minute heating rate, and a 10 min holding. Equipment calibrations were completed using single sugar standards, including rhamnose, arabinose, xylose, glucose, fructose, galactose, and mannose. Inositol, a structural isomer of glucose and sugar alcohol, was used as an endogenous reference (Sigma, Beijing, China) for GC analysis.

2.5. Structural analysis of compounds

Infrared (IR) spectra of garlic supernatant polysaccharide fractions were obtained using a previous approach with an IR spectrometer (VERTEX 70 & HYPERTION Bruker Instrument Co., Ltd., Karlsruhe, Germany) (Wang et al., 2022). For the spectrometry analysis, 1 mg of garlic supernatant polysaccharides were mixed with dry potassium bromide (KBr) in a mortar and ground to a homogenous powder using a pestle. The powder was transferred into a die cavity and spread evenly using a metal spatula. The entire die set was placed into the hydraulic pellet press (Specac® Ltd., London, UK) and pressed at 5 kN to form a pellet by rotating the wheel tightly for 30 s. By adopting OMNIC™ software (Thermo Fisher Scientific, MA, USA), the sample pellet was submitted to the IR spectrometer and its obtained spectrum was analyzed at 16 scans in the 4000–400 cm^{-1} range. We used a KBr pellet with no garlic supernatant polysaccharide sample as a control sample to eliminate background interference in the IR Transparent medium.

An AVANCE™ III HD NanoBAY spectrometer (Bruker Instrument Co., Ltd., Karlsruhe, Germany) was used to record hydrogen (^1H) and carbon-13 (^{13}C), 2D COSY and 2D HSQC nuclear magnetic resonance (NMR) spectra at 600 MHz for the structural characterization of garlic supernatant polysaccharides. We dissolved 60 mg of each polysaccharide sample in 1 mL D_2O (deuterium, 99.8%; Titan Scientific Co., Ltd., Shanghai, China) at 25 °C and incubated for 24 h before analysis. The sample spectrum was obtained at 25 °C after 1024 or 4096 scans, with the 8012 Hz pulse width and the 1.0-s relaxation delays, with chemical shifts (δ) relative to tetramethylsilane (TMS) as an external reference.

2.6. Analysis of viscosity properties of garlic supernatant polysaccharides and dynamic viscoelastic properties of dough samples

A shear rate (γ = 0–100 s^{-1}) sweep test was performed on the polysaccharide solutions using a Brookfield RDVD-II viscometer that contained the CC3-40 cylindrical rotor (Brookfield Engineering, Middleboro, MA, USA) to evaluate apparent viscosity properties of the polysaccharides in garlic supernatant samples. To investigate how the temperature and concentration of samples affect the apparent viscosity of the polysaccharides fractions, we analyzed 90 mg/mL of each sample at 20, 30, 40, 50 and 60 °C and assessed 10, 30, 50, 70, and 90 mg/mL of each sample at 25 °C. Each analysis was conducted in triplicates with the thermostatic water bath as the control temperature (20, 25, 30, 40, 50 and 60 °C). A ChemStation system, Rheo3000, developed by Brookfield Engineering, was employed for data recording and analysis.

Dough was loaded onto the HAAKE MARS-III rheometer (Thermo Fisher Scientific, Waltham, MA, USA) for analysis by using one steel plate (diameter, 20 mm) and one 1 mm gap guard against water loss with mineral oil (Sigma, Beijing, China) to determine the functions of adding garlic supernatant polysaccharides in dough dynamic viscoelastic properties. The dough samples were prepared by mixing 50 g wheat flour with 0, 3, 5, 7, or 10% (*w/w*) of garlic supernatant polysaccharides (based on flour weight) and 50 mL water, kneaded for 5 min at 50 r/min with a dough LAB system (Perten Instruments, Sweden) and then let to stand for 10-min under ambient temperatures. A frequency sweep test was conducted within the 0.1–10 Hz range at 25 °C and the 1% strain amplitude. The temperature of the sweep test was increased from 25 to 95 °C at the 5 °C/min heating rate at the 10 Hz angular frequency together with the 1% strain amplitude. We determined the loss modulus (*G*") along with the storage modulus (*G*') of the samples and displayed their loss tangent (tan δ) as *G*"/*G*'.

2.7. The distribution analysis of the water in dough samples

About 1.5 mg of prepared dough in Section 2.6 were placed into NMR tubes with a 10 mm diameter and then analyzed using an NMI 20 LF-NMR analyzer at 20 MHz (Niumag Co., Ltd., Suzhou, China) to explore the water content and mobility in the dough samples. The sample size was maintained at around 3 cm to evaluate the transverse relaxation time (T_2) signals with the Carr-Purcell-Meiboom-Gill pulse sequence (He, Guo, Ren, Cui, Han & Liu, 2020), with the following settings: 0.02 ms pulse separation, 3000 echoes, 16 scans, 0.5 T magnetic strength, 1.0 s recycle delay, 32 °C temperature, 60 mm coil diameter, 150 data points and 1000 ms for the waiting time between the two measurements. The data points were collected and analyzed using the inbuilt application analysis software (Version 1.0, Niumag Co., Ltd., Suzhou, China).

2.8. Texture characteristics analysis of dough samples

The texture profiles of dough samples prepared in Section 2.6 were evaluated at 25 °C using a Stable Micro Systems TA-XT Analyzer (Stable Micro System, Godalming, UK). and the analysis performed as described previously with a few modifications (Yang, Pan, Li, Li & Li, 2022). A 5.0 g dough measuring 30 × 12 × 12 mm, placed in a mould without deformation was added into an airtight loading platform with 50% relative humidity for 10 min to ensure stable dough properties before tests. Twelve tests were performed on the same dough sample, and triplicate analyses on the different samples. The settings used for the analysis were: P-75 aluminium pressure plate probe, force-distance deformation, 5.0 g trigger force, 1.5 mm/s testing speed, 2.5 mm/s pre- as well as post-test speed, 40% strain, 5 mm return distance, and 5 s waiting time between two measurements. We recorded the elasticity, hardness, resilience, cohesion, and adhesion of the dough samples as the representative parameters of the sample texture.

2.9. Thermal analysis of dough samples

The differential scanning calorimetry (DSC)-60 plus instrument (SHIMADZU Co., Kyoto, Japan) was used to evaluate thermal dough properties, including transformation temperatures and enthalpy change.

Each sample was frozen in liquid nitrogen and vacuum-freeze dried before tests. An aliquot of 3 mg freeze-dried samples was transferred and encapsulated in aluminium pans using a pan press (Shanghai Qunhong Instrument Equipment Co., Ltd, Shanghai, China) and subsequently placed on a constantan disc onto the DSC analysis cell platform. We also placed one empty reference pan on the symmetric platform in the DSC analysis cell as a control and evaluated the levels of heat release and consumption of the samples by comparing the different temperatures of samples with the surrounding media. Each sample was then heated from 30 to 300 °C at 10 °C/min heating rate. We adopted the TA-60 software version 2.21 (SHIMADZU) to record and analyze the initial sample temperature (T_o), peak temperature (T_p), and temperature (T_e), together with enthalpy change (ΔH) in a phase transition.

2.10. IR spectroscopy of gluten proteins from dough samples

We extracted 5 g of gluten by washing the dough samples using 3% NaCl solution (*w/v*) for a 10 min period at 50 mL/min, followed by washing with distilled water for 1 min at 50 mL/min using the MJ-IIIA gluten washing machine (Topp Yunnong Technology Co., Ltd, Zhejiang, China). The samples were then centrifuged for 15 min at 3,400 rpm, dialysed and lyophilized to recover gluten from the eluents.

The spectroscopy was conducted in a VERTEX 70 & HYPERTION IR spectrometer (Bruker Instrument Co., Ltd., Karlsruhe, Germany) to determine the secondary structure of the dough-derived gluten. A 1 mL of lyophilized gluten sample was mixed with 150 mg of dry KBr in a mortar and ground for 2 min to a homogenous powder using a pestle. The powder was transferred into a die cavity and spread evenly using a metal spatula. The entire die set was placed into the hydraulic pellet press (Specac® Ltd., London, UK) and pressed to form a pellet by tightly rotating the wheel at 5 kN for 30 s. The obtained pellet from the die was uploaded to the IR spectrometer to determine its spectrum in the 4000–400 cm^{-1} range at 64 scans. The KBr pellet without dough samples was used as a control sample to eliminate background interference in IR Transparent medium.

We analysed the IR spectra with Peakfit software version 2022 SR1 (OriginLab, Northampton, USA) and OMNIC™ software package (Thermo Fisher) and detected typical absorption peaks for β-sheet at 1610—1640 cm^{-1}, random coil at 1640—1650 cm^{-1}, α-helix at 1650—1660 cm^{-1}, and β-turn at 1660—1670 cm^{-1} range, and calculated their proportions by adopting Gaussian curve fitting model after peak separation through derivative spectrophotometry (De Castro, Sahsah, Heyden, Regalbuto & Williams, 2022).

2.11. Analysis of the microstructure of dough samples and cross-linking effects of polysaccharide fractions on dough network

The microstructure of freeze-dried dough samples supplemented with garlic supernatant polysaccharides was fixed and coated using the thin gold layer with the sputter-coater (ZKY-SBC-12, Ziyuone Technology Co., Ltd., Beijing, China) and then observed under an Apreo 2 Scanning electron microscopy (SEM) system (Thermo Fisher Scientific, MA, USA) with 500×, 1000×, and 10000 × magnifications and images recorded and analyzed.

We used the Nikon Ti-U inverted confocal laser scanning microscopy (CLSM) (Nikon Imaging Japan Inc., Minato-ku, Tokyo) to visualize sample fluorescence dyes to explore garlic supernatant polysaccharides distributions in dough network and determine the cross-linking effects between polysaccharide fractions and dough network. The garlic supernatant polysaccharides and gluten protein samples were stained as described previously with minor modifications (Li, Liu, Wu, Wang & Zhang, 2016). About 30 mg of garlic supernatant polysaccharide samples were activated by adding 200 μL of 0.2 M NaOH and incubating for 12 h. Dialysis was performed overnight on the mixtures using borate saline solution (0.2 M, pH 8.0) to remove residual NaOH, followed by the addition of 6 mg of 5-aminofluorescein to stain 5 mL of the activated garlic supernatant polysaccharide solutions for a 1 h in darkness, and final dialysis using deionized water. The dialysates were freeze-dried in liquid nitrogen and a vacuum. Subsequently, 25 mg of the lyophilized dialysates were blended using 5 g of wheat dough and mixed with 2.5 mL of sterile water before analyses.

A 1 g of dough containing polysaccharides was then collected at the centre of the prepared dough before transferring to a flake-shaped specimen measuring 15 × 15 × 0.8 mm. The gluten in the dough sample was dyed by incubation using 5 μL of rhodamine B (10 μg/mL) for 1 min. The laser excitation wavelength was 488 nm for the fluorescently labelled polysaccharides and 543 nm for stained gluten protein respectively, while their emission wavelengths were 543 and 590 nm, respectively. The dough containing garlic supernatant polysaccharides was added onto the motorized x-y platform, and the constant z-position was used to record digital images with a resolution of 1024 × 1024 pixels and 212 × 212 μm. The features of the obtained dough network in each binary image, including the average size (ΦA, μm^2), area fraction (*AF*, %), fractal dimension (*FD*), perimeter (*P*, μm) and junctions density (*JD*, %), were characterized using the ImageJ tool (ver 1.50b) and AngioTool software (ver 0.6 National Institutes of Health, USA).

2.12. Statistical analysis

At least three parallel experiments were conducted for all the analyses. Data are represented by mean ± standard deviation or mean only. OriginPro 2022 SR1 software (OriginLab Corporation, Northampton, USA) and SPSS 22.0 (IBM, NYS, USA) software were used for statistical data analysis and generations of graphs. Duncan multiple comparisons test, one-way ANOVA, and homogeneity test of variance were used to determine significant differences among groups, with a significance level indicated when $P < 0.05$.

3. Results and discussion

3.1. Compositional analysis

The chemical compositional analysis showed different contents of total sugar and protein (Table 1) among the polysaccharides extracted from SGSOS (Yunnan garlic), HGSOS (Cangshan garlic) and PGSOS (Tianjin garlic). SGSOS fraction had a relatively decreased protein level (0.35%) whereas increased total sugar level (90.91%) relative to HGSOS (1.98% and 84.55% separately) and PGSOS (0.86% and 82.61% separately) fractions. The monosaccharide composition profiles (Table 1) showed that SGSOS, HGSOS and PGSOS fractions mainly comprised

Table 1
Chemical analysis and molecular weight distribution of the garlic supernatant polysaccharides.

	sample		
	SGSOS	HGSOS	PGSOS
Chemical composition			
Total sugar content (%)	90.91 ± 0.15^a	84.55 ± 0.09^c	82.61 ± 0.03^c
Protein content (%)	0.35 ± 0.18^f	1.98 ± 0.07^b	0.86 ± 0.14^d
Molecular weight distribution			
$M_n/10^3$ Da	2.20	2.10	2.10
$M_w/10^3$ Da	3.00	2.90	2.90
Monosaccharide composition			
Rhamnose	29.94	–	85.82
Glucose (G)	39.41	67.14	9.96
Fructose (F)	30.65	32.86	4.21
G:F	1.29^c	2.04^b	2.37^a

Note: SGSOS, HGSOS and PGSOS are polysaccharides fractions collected in Yunnan, Cangshan and Tianjin garlics. The weight average molecular weight (*M*w) is calculated by dividing total sample mass by weight fraction in each polysaccharide, whereas number average molecular weight (*M*n) is calculated by overall molecular number within each sample. Different letters in the same line indicated significant difference ($P < 0.05$).

glucose and fructose with a considerable proportion of rhamnose in SGSOS (29.71%) and PGSOS (39.44%) fractions. HGSOS fractions had the highest glucose level (68.30%), followed by the fractions of SGSOS (39.53%) and PGSOS (21.96%). The fructose level was highest among the fractions from PGSOS (38.60%) and lowest in SGSOS (30.76%) (Table 1).

A significantly lower ratio of glucose (*G*) level to fructose (*F*) was observed for SGSOS (1.29) fraction compared with HGSOS (2.04) and PGSOS (2.37) fractions. The garlic polysaccharide fractions have been found to consist primarily of glucose and fructose, corroborating our findings. Glucose residue exists in garlic polysaccharide fractions, mainly as a ketose resulting in a molecular chain of its units (Ni, Xu, Zhu, Pang, Lv & Mu, 2021). The steric hindrance of the molecular chain of garlic polysaccharides is also enhanced with an increase in glucose substituents. This implies that the SGSOS fraction may have a lower steric hindrance of the molecular chain, resulting in a relatively higher molecular flexibility, which improved the ability of glucose units to cross-link and form a relatively large molecule. Low rhamnose content has also been reported in garlic polysaccharide fractions (Diretto, Rubio-Moraga, Argandona, Castillo, Gomez-Gomez & Ahrazem, 2017). However, its presence in SGSOS and PGSOS fractions may be attributed to different growing conditions or varieties of garlic. Rhamnose has several health benefits associated with the increased glycemic index of rhamnose compared to glucose and fructose (Guo, Yin, Cheng, Chen & Ye, 2022). The difference in the monosaccharide composition among the fractions is a also critical factor indicating polysaccharide physicochemical characteristics.

3.2. Molecular weight of polysaccharide fractions

Our data showed relatively high *M*n (2.20×10^3 Da) and *M*w (3.00×10^3 Da) in SGSOS fraction compared to HGSOS and PGSOS fractions (*M*w 2.90×10^3 and 2.10×10^3 Da) (Table 1). The molecular weight can influence the physicochemical characteristics of garlic supernatant polysaccharide fractions, such as swelling capacity, and molecular cross-linking degree(Qiu, et al., 2022).

3.3. Garlic supernatant polysaccharide structures

The IR and NMR spectroscopy were conducted to reveal the structural characterization of garlic supernatant polysaccharides. The results showed that SGSOS, HGSOS and PGSOS fractions comprised neutral

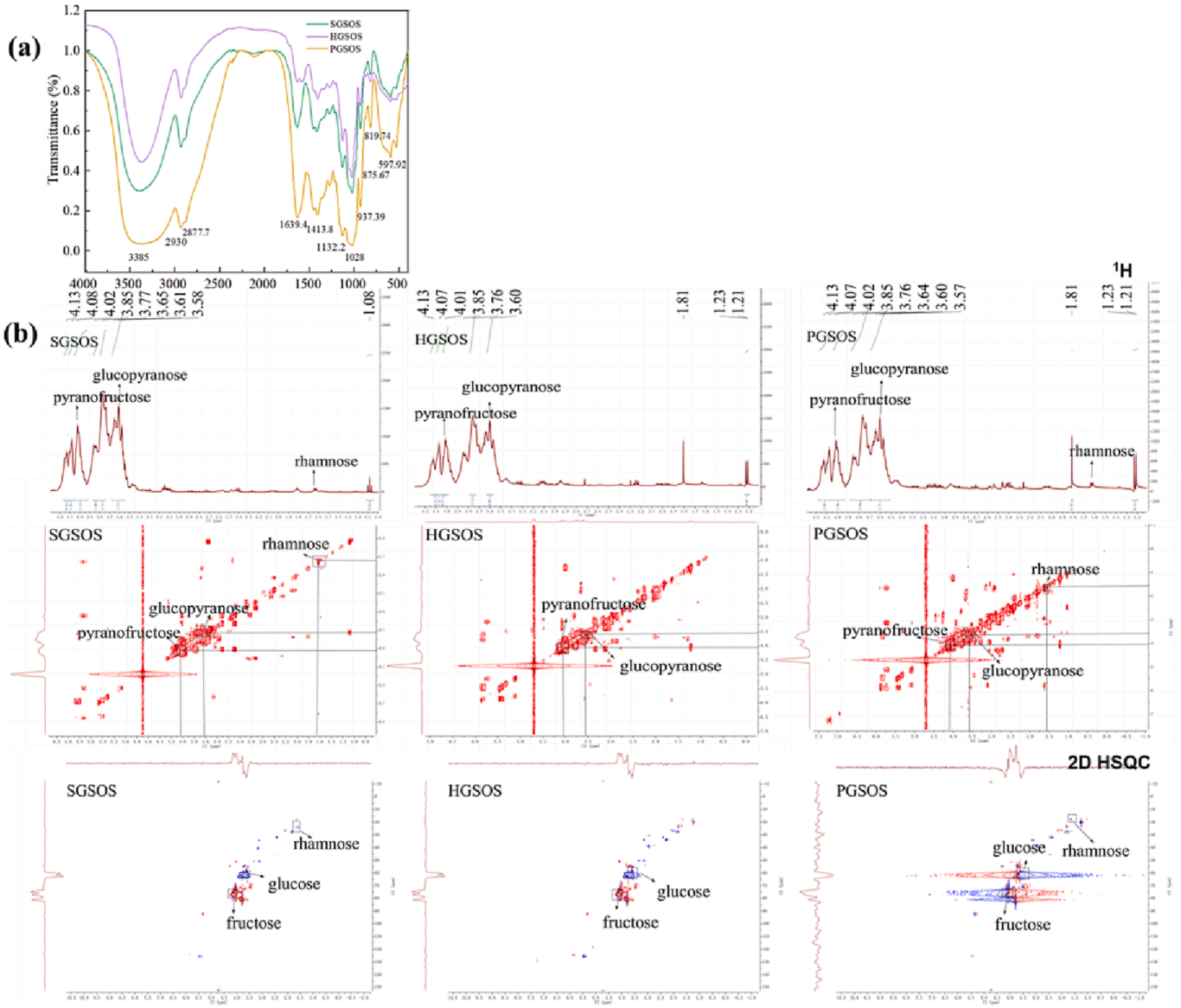

Fig. 1. Infrared (IR) (a) and nuclear magnetic resonance (NMR) spectroscopy on garlic polysaccharides within D_2O (b).

polysaccharides, evidenced by a lack of peaks at 1483–1431 or 1573–1506 cm^{-1} on IR spectra (Fig. 1a). This finding is consistent with the absence of peaks at 172.35 ppm and 178.22 ppm in the ^{13}C NMR spectra (Fig. 1b), which also represents lack of gluconic acid. Typical insulin absorption bands (near 937, 820 and 598 cm^{-1}) were observed on the IR spectra (Vazquez-Vuelvas, Chavez-Camacho, Meza-Velazquez, Mendez-Merino, Rios-Licea & Carlos Contreras-Esquivel, 2020), with characteristic signal peaks of glucopyranose near δ 3.6 ppm and pyranofructose (between δ 3.8 and δ 4.2 ppm) in the NMR spectra of all the polysaccharide fractions, and rhamnose near δ 1.3 ppm on NMR spectra of SGSOS and PGSOS fractions, conforming to the monosaccharide compositional analysis (Wang, et al., 2023). The signal peaks below 4.95 ppm in the ^{1}H NMR, and between δ 103 ppm and δ 104 ppm in the ^{13}C NMR spectra represented the β-configuration for glycoside (Xu, Yang, Yang, Feng, Jiang & Zhang, 2017), indicating that β-pyranose was the most abundant monosaccharide residue within the garlic supernatant polysaccharides.

3.4. Apparent viscosity of garlic supernatant polysaccharides

Garlic supernatant polysaccharide solutions displayed the shear-thinning behaviour of non-Newtonian fluids (Fig. 2a) (Guo, Ma, Cai & Huang, 2023). The apparent viscosity exhibited a gradual decline and stabilization trend as shear time elevated. The apparent viscosity of the polysaccharide solutions gradually increased as the concentration of the solutions increased from 10 to 90 mg/mL and as the temperature decreased from 60 to 20 °C. These observations could be due to the enhanced attractive forces between molecules at high concentrations of polysaccharides or low temperatures (Zang, et al., 2022). The attractive force between molecules increased with increased in concentration of the solutions or decreased temperature probably due to the reduced intermolecular distance or relative motion. The augmented apparent viscosity was observed for SGSOS compared to HGSOS and PGSOS fractions at the same temperature and solution concentrations. Such a difference could be explained by the relatively higher *M*w (3.00×10^3

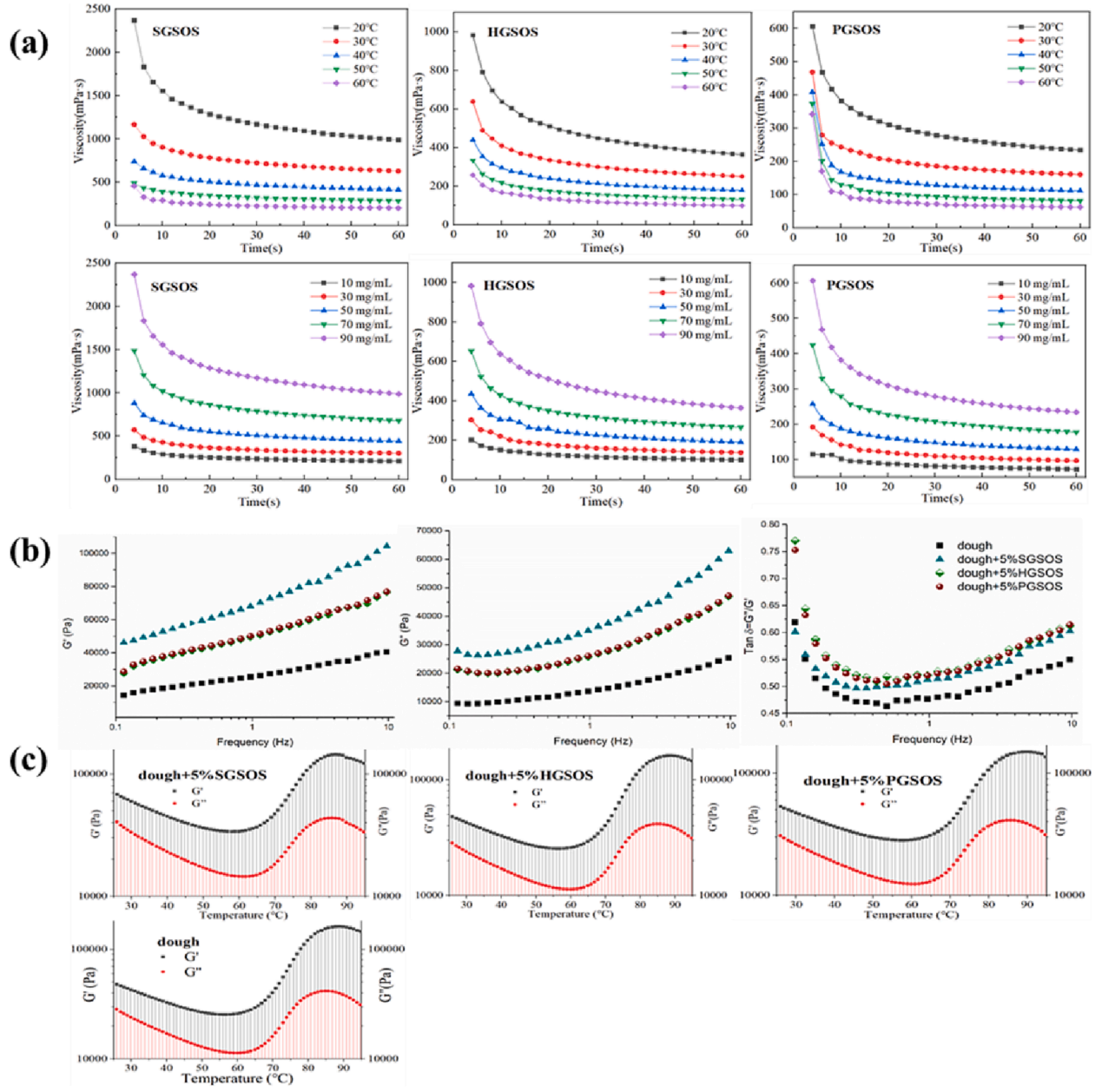

Fig. 2. Apparent viscosity of garlic polysaccharide (a) and the viscoelasticity of fortified dough using frequency sweep (25 °C) (b), and stability profiles using temperature sweep (-25–95 °C) (c).

Da) or *M*n (2.20×10^3 Da) of the SGSOS fraction compared to low values of *M*w and *M*n those of HGSOS and PGSOS fractions (*M*w value = 2.90×10^3 Da and *M*n value = 2.10×10^3 Da, independently). Previous studies report that a long molecular chain is correlated with a low mobility rate of a molecular segment, which could explain the stronger chain flexibility and increase the cross-linking effect between molecules. Lower glucose substituents in SGSOS fraction may also promote stronger chain flexibility. These features have an important impact on enhancing the interaction between polysaccharide fractions and other food components (Shao, et al., 2022).

Despite having the same molecular weights, the apparent viscosity was slightly reduced in the PGSOS fraction compared with the HGSOS fraction. This can be attributed to the lower chain flexibility and decreased ability of the interconnection for a comparatively large fragment due to the steric hindrance caused by rhamnose substituent groups as side chains.

3.5. Effects of garlic supernatant polysaccharides on moisture distribution in doughs

Moisture distribution has an important influence in determining the properties of dough, such as rheological character and texture characteristics of dough during processing. Therefore, we analyzed the moisture distribution in fortified dough and found peaks T_{21} (0–0.98 ms), T_{22} (1.12–9.78 ms) and T_{23} (13.34–103.08 ms) (Table 2) on LF-NMR spectra to be associated with bound water (intra-granular water of molecules in dough), immobilized water (water populations onto molecule surface in dough), and free water (free-moving water dissociated from molecules in dough), respectively (Xiao, Ding, Cheng, Xu & Lin, 2022). The bound and immobilized water plays an important role in the swelling ability of gluten or starch molecules, thus promoting dough development. We used the relaxation time and percentage peak areas to quantify water mobility and the relative content of the water population, respectively, with higher T_2 values indicating stronger water mobility and higher area proportions of peaks meaning a high percentage of the corresponding water.

Peaks T_{21} and T_{22} in fortified doughs with 3, 5, 7 and 10% garlic supernatant polysaccharide fractions (SGSOS, HGSOS and PGSOS) distinctly showed an increase in the relaxation time and corresponding peak areas, compared with control dough samples (Table 2). Therefore, adding garlic supernatant polysaccharides could combine the bound and immobilized water with gluten matrix or starch granules, thus favouring the formation of dough network structure. This can also be explained by stronger or more stable interactions of the garlic supernatant polysaccharides with gluten matrix or starch granules through stronger or more stable interaction (Li, Liu, Zheng, Hong, Bian & Li, 2021). On the contrary, the relaxation time and peak areas of the T_{23} decreased for fortified doughs, suggesting weakened mobility or decreased relative content of free-moving water. This observation can be caused by the enhanced hydrophilic interaction of the dough network induced by the connection of garlic supernatant polysaccharide fractions with gluten matrix or starch granules (Gu, Qian, Sun, Wang & Ma, 2023). Dough prepared using 5% SGSOS fraction exhibited the greatest relative content of bound water and the lowest relative content of the free-moving water, as shown by the highest peaks areas of T_{21}, together with the lowest proportions for peak T_{23}, compared to control dough and the samples fortified using the other polysaccharides (Table 2). These behaviours could be conducive to frozen dough processing by inhibiting the growth and recrystallization of ice (Sun, et al., 2023). Adding SGSOS at 5% to doughs could result in mild interaction with the dough network, causing water to be redistributed to maintain its sufficient supply to gluten matrix and starch granules, to form a fully stretched dough structure. However, a similar trend of bound water or free-moving water was not observed in other fortified dough, indicating that the moderate interaction depends on some intramolecular features, such as monosaccharide residues, molecular size or steric hindrance of molecular chain (Table 1) and content of garlic supernatant polysaccharides added to wheat flour. Bound water was not detected in the fortified dough at 10%, possibly due to the competitive water absorption of garlic supernatant polysaccharides in the dough network.

3.6. Effects of garlic supernatant polysaccharides on texture characteristics of doughs

The texture characteristics of fortified dough prepared with garlic supernatant polysaccharides were closely associated with the dough network but significantly differed from the control dough samples (Table 3). Fortified dough samples had higher elasticity and cohesion than the control dough, with the highest changes observed in hardness and chewiness when 5% (w/w) garlic supernatant polysaccharides fractions were added to the dough ($P < 0.05$). The dough samples supplemented with 10% (w/w) garlic supernatant polysaccharides also displayed the highest hardness and chewiness levels but showed lower elasticity, cohesion and adhesion. We speculate that the moderate molecular characteristics and 5% of garlic supernatant polysaccharides the cross-linking activity of the dough network. Excess garlic supernatant polysaccharides excessively compete for water molecules, leading to water loss from the dough network and the hardening of its structure, thereby inhibiting the development of the gluten network as well and impairing starch and protein hydration during processing, resulting in the dough with diminished volume, poor taste and tough texture. The hydrophilic group in polysaccharides could also have been improved by

Table 2
Relaxation times T_2 and corresponding peak areas analysis of dough samples.

Sample	addition (%)	T_{21}		T_{22}		T_{23}	
		Time (ms)	Area (%)	Time (ms)	Area (%)	Time (ms)	Area (%)
dough	0	0.19	0.60	6.14	97.60	174.75	1.80
+SGSOS	3	0.19	0.70	6.80	98.00	151.99*	1.30
	5	0.22	5.11*	9.33*	94.00*	114.98*	0.89*
	7	–	–	6.14	98.00	151.99*	2.00
	10	–	–	8.52*	98.30	114.98*	1.70
+HGSOS	3	–	–	7.06	98.40	159.58*	1.60
	5	0.19	4.04*	10.72*	94.41	120.72*	1.55
	7	0.27	2.94*	6.14	94.84*	145.05*	2.13*
	10	–	–	7.06	96.70	86.98*	3.30*
+PGSOS	3	–	–	8.11*	98.51	174.75	1.49
	5	0.29	3.98*	8.92*	94.30*	114.98*	1.72
	7	0.19	1.09	6.14	97.41	132.19*	1.99
	10	–	–	9.33*	98.10	114.98*	1.90

Note: Data are presented as the mean (n = 3); -, represent no detected. T_{21}, T_{22} and T_{23} are the relaxation time of bound water, immobilized water, and free water. * in the same column represent significant difference ($P < 0.05$).

Table 3
Results from TPA analysis, DSC analysis, IR and CLSM micrographs of doughs.

Sample	dough	dough + 5 % SGSOS	dough + 5 % HGSOS	dough + 5 % PGSOS
Texture profile				
Hardness	188.10 ± 1.00^{a}	85.42 ± 1.17^{c}	73.95 ± 4.63^{d}	54.58 ± 4.75^{d}
Elasticity	0.36 ± 0.08^{d}	0.86 ± 0.09^{a}	0.84 ± 0.11^{a}	0.74 ± 0.17^{a}
Gumminess	0.38 ± 0.06^{c}	0.80 ± 0.04^{a}	0.68 ± 0.02^{a}	0.66 ± 0.11^{a}
Chewiness	15.36 ± 3.83^{d}	36.63 ± 7.23^{b}	32.60 ± 5.60^{b}	30.45 ± 1.77^{b}
Thermodynamic properties				
T_p (°C)	219.85^{b}	244.24^{a}	236.59^{a}	222.00^{b}
T_o (°C)	150.00^{a}	154.27^{a}	147.78^{a}	146.41^{a}
ΔH (J/g)	−619.48^{c}	−1510.00^{a}	−676.68^{b}	−666.86^{b}
Secondary structure of gluten from IR spectroscopy				
α-Helical	25.58 ± 0.32^{a}	24.38 ± 2.52^{a}	24.08 ± 1.31^{a}	23.83 ± 2.09^{b}
β-sheet	27.34 ± 1.51^{b}	33.21 ± 3.66^{a}	32.15 ± 3.51^{a}	32.10 ± 4.24^{a}
β-turn	25.98 ± 0.36^{a}	22.63 ± 1.85^{c}	23.45 ± 1.35^{b}	22.44 ± 2.22^{c}
random coil	21.10 ± 1.11^{a}	19.97 ± 1.17^{b}	20.31 ± 1.40^{a}	20.63 ± 2.60^{a}
Parameters related to dough network analyzed from CLSM micrographs				
average size (ΦA, μm^2)	268.6 ± 1.35^{d}	994.76 ± 2.78^{a}	356.92 ± 4.41^{b}	333.19 ± 3.28^{c}
area fraction (AF, %)	50.65 ± 1.07^{b}	68.55 ± 1.31^{a}	67.06 ± 2.05^{a}	65.34 ± 1.01^{a}
perimeter (P, μm)	26.82 ± 0.49^{c}	43.77 ± 1.94^{a}	29.34 ± 0.58^{b}	27.55 ± 2.56^{c}
fractal dimension (FD)	1.80 ± 0.04^{a}	1.64 ± 0.04^{b}	1.75 ± 0.04^{a}	1.78 ± 0.04^{a}
junctions density (JD, %)	10.8 ± 0.20^{d}	20.1 ± 0.02^{a}	16.3 ± 0.25^{b}	12.2 ± 0.10^{c}

Note: Dates are presented as the mean ± SD (n = 3). Different letters in the same line indicated significant differences between groups ($P < 0.05$).

the combination of water with gluten matrix or starch granules.

The 5% garlic supernatant polysaccharides were supplemented by wheat flour during the dough preparation for subsequent experiments to maximize garlic polysaccharides role in the dough micro- and mesoscopic characteristics.

SGSOS-fortified dough showed relatively higher values of Texture Profile Analysis (TPA) profiles than HGSOS and PGSOS-fortified doughs, probably due to the slightly higher contents of immobilized and bound water in SGSOS-fortified doughs and the somewhat stronger cross-linking between SGSOS and dough network and reinforced dough structure. These effects are highly dependent on the inherent features of the polysaccharide molecule, including monosaccharide residue, molecular flexibility (steric hindrance of the molecular chain represented by *G:F* ratio), and molecular weight (Collar, Villanueva & Ronda, 2020). This implies that the molecular interaction between SGSOS and gluten matrix or starch granules was more effective and was caused by the higher molecular flexibility of the SGSOS fraction. The findings also imply that SGSOS interacted with gluten matrix or starch granules without competing for water, thus forming a moderate dough network (Liao, Zhang, Jiang, Javed, Xiong & Liu, 2022). In contrast, HGSOS- and PGSOS-fortified doughs created a comparatively rigid structure due to their lower molecular weight or higher steric hindrance in the molecular chain, inducing inadequate cross-linking between polysaccharides and the dough networks. This finding was verified by lower elasticity and gumminess values of HGSOS- and PGSOS-enriched doughs compared with SGSOS-enriched dough.

3.7. Roles of garlic supernatant polysaccharides in dough thermodynamic properties

We determined the thermal stability analysis of the different garlic supernatant polysaccharides and fortified doughs by the DSC method, with SGSOS fraction showing significantly higher T_P, T_o, and ΔH in a phase transition ($P < 0.05$) (Table 3), indicating higher thermal stability in SGSOS fraction compared to HGSOS and PGSOS fractions. The high T_P value for the SGSOS fraction may be due to the relatively strong inherent molecular features or intermolecular forces such as hydrophobic interaction.

The fractions of SGSOS-, HGSOS- and PGSOS-fortified dough samples exhibited relatively higher ($P < 0.05$) T_P and ΔH and in-phase transition than that of the control doughs, indicating that the addition of garlic polysaccharide fractions into dough causes a compact and uniform dough network structure, especially for the SGSOS fraction. However, no significant differences ($P < 0.05$) between T_P and T_o were observed in the fortified dough samples. This implies that supplementing a dough with garlic supernatant polysaccharides made no obvious change in heat requirement during the phase transition. It is beneficial since it conserves energy because no increase in heat is required during processing (Mao, Gao & Meng, 2023). The higher ΔH in the SGSOS-fortified doughs confirms that the addition of SGSOS results in a moderate interaction between polysaccharides and gluten matrix or starch granules because of the increased molecular flexibility, thereby bring the strengthening the dough network structure.

3.8. Dynamic viscoelastic properties of fortified dough samples

We observed the impacts of 0–10% garlic supernatant polysaccharides on the viscoelastic profiles using frequency sweep and stability profiles using temperature sweep. Frequency sweep test results showed an increase in *G*' for the fortified dough samples, whereas *G*" was detected at a higher frequency, which is consistent with the solid-like characteristics of dough. The garlic supernatant polysaccharides also increased *G*' and *G*" in doughs, especially for SGSOS at 5% (Fig. S1and Fig. 2b).

These findings are consistent with the results on moisture distribution in fortified dough samples and TPA profiles, implying that SGSOS fraction adequately interacted with the gluten matrix or starch granules to improve the formation of a more orderly and elastic-like structure with increased plasticity (Yazar & Demirkesen, 2022).

A tan $\delta < 1$ (G" < G') indicates no change in the overall elastic-like behaviour of fortified dough (Liu, McClements, Li, Xiong & Sun, 2019). The 5% garlic supernatant polysaccharides-fortified dough displayed enhanced tan δ level, whereas the frequency dependency decreased compared to the control dough. The garlic supernatant polysaccharides also did not reduce the elasticity and viscosity of the dough, probably due to the moderate cross-linking affinity between the polysaccharides (5%) and the dough network (Zhou, Dhital, Zhao, Ye, Chen & Zhao, 2021). The binding between water and other dough components may not have also been influenced, causing a fair viscoelastic behaviour of dough, probably because of the trapped water in garlic supernatant polysaccharide fractions at a moderate level, especially for SGSOS fraction at a proportion of 5% in the dough.

The *G*' and *G*" of the doughs initially decreased, then increased and finally declined for the temperature sweep test (Fig. 2c). The increased *G*" or *G*' levels from 25 to 60 °C possibly occurred due to the enlarged gluten network and the relative sliding resulting from molecular thermodynamic movement or water dissociation, leading to a relatively reduced strength of the dough network structure (Liang, Shi, Shi & Cao, 2023). However, cross-linking and molecular chain coils may be responsible for the increased *G*' and *G*" from 60 to 80 °C (Mao, et al., 2022). The doughs had maximum *G*' and *G*" values at 85 °C, implying a larger dough network construction at this temperature. At temperatures above 85 °C, *G*' and *G*" rapidly decreased, probably due to the shrinking

of the dough network caused by protein denaturalization or starch gelatinization.

A 5% SGSOS-fortified dough exhibited relatively high dynamic moduli (Fig. 2b) and lower temperature dependence (Fig. 2c), which may be due to the cross-linking of the garlic supernatant polysaccharides on the dough network, ultimately increasing its stability and inhibiting protein denaturation and starch gelatinization. This observation can be attributed to the intrinsic molecule features of garlic supernatant polysaccharides, including the relatively high molecular weight and lower steric hindrance of the molecular chain, which may affect the cross-linking between garlic supernatant polysaccharides and the dough network (Tolstoguzov, 2000).

3.9. Effects of garlic supernatant polysaccharides on the protein structure of doughs

Our data showed a high correlation between the protein secondary structure is presented in Table 3. The protein structures with the establishment and strength of the dough network (Table 3). Fortified doughs demonstrated a relatively higher percentage of β-sheet structure than the control doughs, with the highest in 5% SGSOS-fortified dough (,33.21%), lower α-helix structure and reduced contents of β-turn structure (Table 3). However, the percentages of random coil structures varied, with the lowest in SGSOS (19.97%) followed by the control dough (21.10%), PGSOS (22.44%) and HGSOS (23.45%). β-sheet and α-helix motifs correspond to relatively orderly and stable protein structures (Wang, et al., 2022), and their predominance in SGSOS-fortified dough could be due to higher hydrogen bond proportion between the dough network and garlic supernatant polysaccharides, indicating the formation of relatively strong and ordered gluten networks in the fortified doughs.

The increase in the formation of β-sheet conformation, described as the relatively stabilized structure, at cost of β-turn and random coil conformation in SGSOS-enriched dough sample and at the cost of β-turn and α-helix conformation in PGSOS- and HGSOS-enriched dough samples (Nhouchi, Botosoa, Chene & Karoui, 2022). These results are consistent with previous findings that SGSOS fraction effectively interacted with gluten matrix or starch granules due to its relatively high molecular weight and relatively low steric hindrance of the molecular chain, which may be advantageous to the intrinsic organization or strength of the gluten network.

3.10. Microstructure of fortified doughs and molecular interaction

We explored the microstructures of the fortified doughs using SEM and CLSM (Fig. 3b) to assess the cross-linking of garlic supernatant polysaccharide fractions on dough network.

The analysis of SEM images showed different morphologies of the polysaccharide-containing doughs than the control doughs (Fig. 3a and S2) with the 5% SGSOS-fortified dough exhibiting a relative rise in surface harshness and the number of apertures compared to the controls. These effects can result in enhanced gas retention ability and desirable quality, minimizing the formation of an excessively compact gluten matrix, reduced volume and rock-hard texture (Lafiandra, Sestili, Sissons, Kiszonas & Morris, 2022). The effect can also be due to the bridging of other constituents in the dough network by the hydrophilic polysaccharide fractions to build a stronger three-dimensional network. The evidence for a stronger interaction between the SGSOS fraction and gluten matrix was indicated by a yellow colour in the SGSOS-fortified dough sample. These characteristics may result in a relatively stable

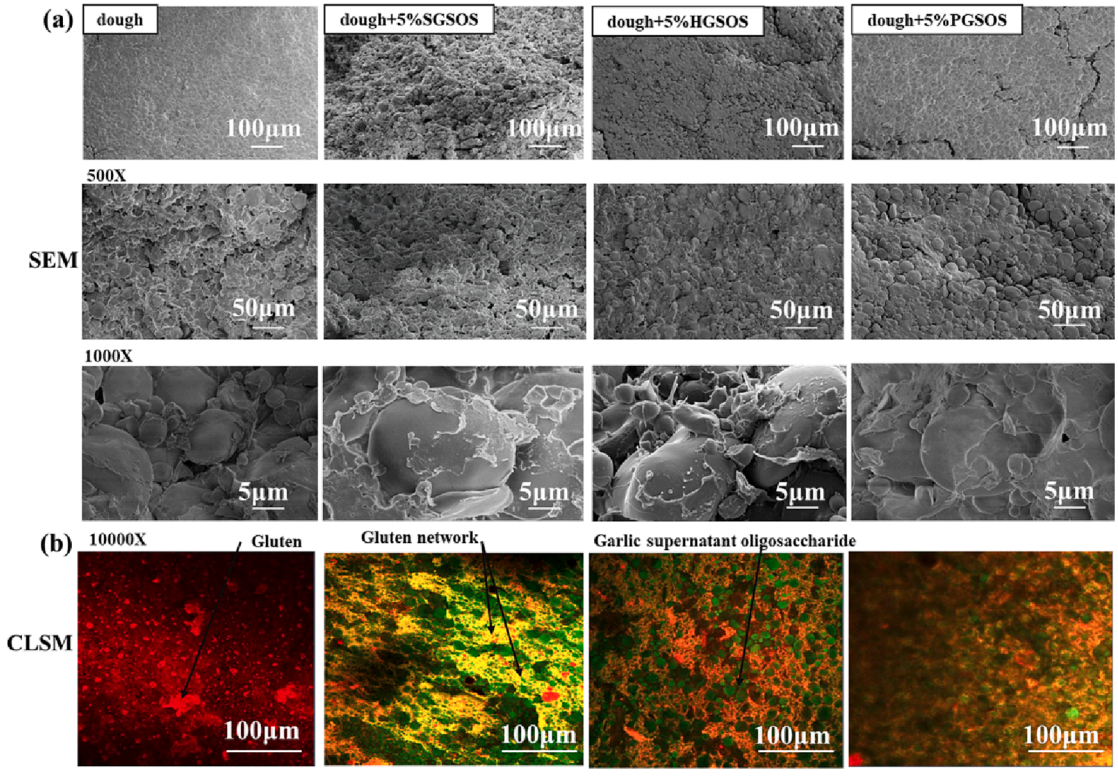

Fig. 3. The scanning electron microscopy (SEM, a) with 500×, 1000×, and 10000 × magnifications and confocal laser scanning microscopy (CLSM, b) observations on fortified dough prepared using 5% garlic polysaccharides. Gluten is represented in red, while garlic polysaccharides in green. The gluten network constructed because of gluten-garlic polysaccharides interaction is denoted as yellow. (For interpretation of the references to colour in this figure legend, the reader is referred to the web version of this article.)

structure and a potential increase in processing adaptability. SGSOS had a fairly long chain and low glucose substituents degree and exhibited stronger chain flexibility and moderate cross-linking, which effectively caused more cross-linking of wheat gluten with SGSOS fraction than with HGSOS and PGSOS fractions.

Analysis of CLSM images (Fig. 3b) revealed distinct microstructures in the polysaccharide-containing doughs, which affect their processing adaptability and quality, unlike the control doughs, which only displayed relatively scattered protein (red) signals. The 5% SGSOS-fortified dough had a well-constructed network structure with increased *ΦA*, *P*, *AF*, and *JD* and decreased dough network *FD* than the controls (Table 3), indicating its relatively stronger associations with gluten. However, the gluten in doughs fortified with HGSOS and PGSOS fractions exhibited a relatively dispersive state and weak fluorescence intensity, indicating their relatively weak cross-linking effects with gluten due to their relatively low *ΦA*, *AF*, *P* and *JD* and increased dough network *FD*. These findings imply that the inherent structural characteristics of the polysaccharides, such as sugar residue composition, M_W or steric hindrance of the molecular chain, play important roles in restructuring the fine-structure of dough connectivity and compactness by enhancing different cross-linking effects between garlic supernatant polysaccharides and gluten. As a result, these characteristics affect the processing adaptability and quality of the dough. As displayed in the graphical abstract, garlic supernatant polysaccharide fractions with higher M_W, as well as lower steric hindrance of the molecular chain, may have a relatively strong capacity to achieve effective gluten protein cooperation, thereby improving structural compatibility between dough network and garlic supernatant polysaccharides fractions. However, garlic supernatant polysaccharide fractions with lower M_W, and higher steric hindrance of the molecular chain could have a relatively weak cross-linking effect on the dough network. This could be explained by distinct molecular crosslinking reaction induced by different molecular chain flexibility depending on inherent molecular characteristics. The polysaccharide fractions with higher molecular weight or lower steric hindrance of the molecular chain can intertwine and form larger network structures due to their enhanced molecular chain flexibility.

Because the cross-linking effects between garlic supernatant polysaccharides and gluten in the dough can change the processing adaptability or quality of garlic polysaccharides-enriched flour products, we investigated the changes in the texture, tensile strength and cooking properties of noodles containing 5% garlic supernatant polysaccharides (Table S1 and Fig. S3). The SGSOS-containing noodles showed significantly higher elasticity, gumminess, chewiness, and tensile distance values, with lower tensile strength ($P < 0.05$) than the controls. These results can be due to the easiness and adequacy of SGSOS to cross-link with the gluten matrix in dough because of its molecular features, forming a firmer gluten network. The SGSOS-enriched noodles also displayed a relatively lower proportion of cooking loss than HGSOS and PGSOS-enriched noodle. Our findings showed that the moderate interaction of the garlic supernatant polysaccharides enhanced the dough network processing, adaptability and quality of the noodles supplemented with garlic supernatant polysaccharides.

4. Conclusions

The present study has exhaustively explored garlic supernatant polysaccharides' cross-linking effect on the dough network by evaluating their physicochemical properties, including sugar residue composition, molecular weight distribution, and steric hindrance of the molecular chain. The findings demonstrated that the SGSOS fraction, with a slightly higher molecular weight ($\sim 10^3$ Da) and lower ratio between glucose and fructose, had the highest compatibility with the gluten matrix than the other garlic supernatant polysaccharide fractions. These features of SGSOS fraction could modify the rheological, thermodynamic textural characteristics and water distribution of doughs. The findings also revealed the connection between the inherent structures of garlic polysaccharides and their impacts on the micro- and mesoscopic characteristics of dough samples. The SGSOS fraction was positively correlated with enhanced strength and firmness of the dough network due to the high capacity to cooperate with the gluten matrix. This implies that a moderately increased molecular size of garlic polysaccharides with relatively low steric hindrance (represented by a lower G:F ratio) of molecular chains effectively increases molecular flexibility and intermolecular forces. These findings provide information on the use of garlic polysaccharides during the processing and manufacturing of foods to enhance their processing adaptability and qualities. Additionally, the investigating approaches might promote the great prospective of non-starch polysaccharides products.

Funding

This work was supported by the project of the National Natural Science Foundation of China (No. 32172169), Tianjin "131" Innovative Talent Team Project (No. 201926).

Declaration of Competing Interest

The authors declare that they have no known competing financial interests or personal relationships that could have appeared to influence the work reported in this paper.

Data availability

Data will be made available on request.

Acknowledgements

Our thanks should go to Instrument and Analysis Center from Tianjin University, Tianjin University of Science and Technology, as well College of Food Science and Bioengineering from Tianjin Agricultural University for their assistance in experiments.

Appendix A. Supplementary data

Supplementary data to this article can be found online at https://doi.org/10.1016/j.fochx.2023.100757.

References

Bozkurt, S., Gorguc, A., Gencda, E., Elmas, F., Koc, M., & Yilmaz, F. M. (2023). Principles and recent applications of vacuum technology in the processing of dough-based cereal products: A comprehensive review. *Food Chemistry, 403*(1), Article 134443. https://doi.org/10.1016/j.foodchem.2022.134443

Collar, C., Villanueva, M., & Ronda, F. (2020). Structuring diluted wheat matrices: Impact of heat-moisture treatment on protein aggregation and viscoelasticity of hydrated composite flours. *Food and Bioprocess Technology, 13*(3), 475–487. https://doi.org/10.1007/s11947-020-02406-z

De Castro, L., Sahsah, D., Heyden, A., Regalbuto, J., & Williams, C. (2022). Dilute limit alloy Pd-Cu bimetallic catalysts prepared by simultaneous strong electrostatic adsorption: A combined infrared spectroscopic and density functional theory investigation. *Journal of Physical Chemistry C, 126*(27), 11111–11128. https://doi.org/10.1021/acs.jpcc.2c00234

Diretto, G., Rubio-Moraga, A., Argandona, J., Castillo, P., Gomez-Gomez, L., & Ahrazem, O. (2017). Tissue-specific accumulation of sulfur compounds and saponins in different parts of garlic cloves from purple and white ecotypes. *Molecules, 22*(8), 1359. https://doi.org/10.3390/molecules22081359

Falsafi, S. R., Maghsoudlou, Y., Aalami, M., Jafari, S. M., Raeisi, M., Nishinari, K., & Rostamabadi, H. (2022). Application of multi-criteria decision-making for optimizing the formulation of functional cookies containing different types of resistant starches: A physicochemical, organoleptic, in-vitro and in-vivo study. *Food Chemistry, 393*(1), Article 133376. https://doi.org/10.1016/j.foodchem.2022.133376

Gu, Y., Qian, X., Sun, B., Wang, X., & Ma, S. (2023). Effects of gelatinization degree and boiling water kneading on the rheology characteristics of gluten-free oat dough. *Food Chemistry, 404*(1), DOI:10.1016/j.foodchem.2022.134715. https://doi.org/10.1016/j.foodchem.2022.134715.

Guo, D., Yin, X., Cheng, H., Chen, J., & Ye, X. (2022). Fortification of Chinese steamed bread with flaxseed flour and evaluation of its physicochemical and sensory

properties. *Food Chemsitry: X, 13*(1), Article 100267. https://www.sciencedirect.com/journal/food-chemistry-x.
Guo, Y., Ma, H., Cai, W., & Huang, Q. (2023). Oxidized yeast β-glucan: Rheological behaviors and the formation of entanglement network at different oxidation degree. *Food Hydrocolloids, 137*(1), Article 108363. https://doi.org/10.1016/j.foodhyd.2022.108363
He, Y., Guo, J., Ren, G., Cui, G., Han, S., & Liu, J. (2020). Effects of konjac glucomannan on the water distribution of frozen dough and corresponding steamed bread quality. *Food Chemistry, 330*(1), Article 127243. https://doi.org/10.1016/j.foodchem.2020.127243
Lafiandra, D., Sestili, F., Sissons, M., Kiszonas, A., & Morris, C. F. (2022). Increasing the versatility of durum wheat through modifications of protein and starch composition and grain hardness. *Foods, 11*(22), 1532. https://doi.org/10.3390/foods11223660
Li, J., Li, J., Jiang, S., Zhao, L., Xiang, L., Fu, Y., … Chen, X. (2023). Addition of Psathyrostachys huashanica HMW glutenin subunit expresses positive contribution to protein polymerization and gluten microstructure of receptor wheat. *Food Chemistry, 405*(Part A), Article 134739. https://doi.org/10.1016/j.foodchem.2022.134739
Li, M., Liu, C., Zheng, X., Hong, J., Bian, K., & Li, L. (2021). Interaction between A-type/B-type starch granules and gluten in dough during mixing. *Food Chemistry, 358*(1), Article 129870. https://doi.org/10.1016/j.foodchem.2021.129870
Li, Q., Liu, R., Wu, T., Wang, M., & Zhang, M. (2016). Soluble dietary fiber fractions in wheat bran and their interactions with wheat gluten have impacts on dough properties. *Journal of Agricultural and Food Chemistry, 64*(46), 8735–8744. https://doi.org/10.1021/acs.jafc.6b03451
Liang, F., Shi, Y., Shi, J., & Cao, W. (2023). Exploring the binding mechanism of pumpkin seed protein and apigenin: Spectroscopic analysis, molecular docking and molecular dynamics simulation. *Food Hydrocolloids, 137*(1), Article 108318. https://doi.org/10.1016/j.foodhyd.2022.108318
Liao, G., Zhang, H., Jiang, Y., Javed, M., Xiong, S., & Liu, Y. (2022). Effect of lipoxygenase-catalyzed linoleic acid oxidation on structural and rheological properties of silver carp (Hypophthalmichthys molitrix) myofibrillar protein. *Lwt-Food Science and Technology, 161*(1), Article 113388. https://doi.org/10.1016/j.lwt.2022.113388
Liu, C., McClements, D. J., Li, M., Xiong, L., & Sun, Q. (2019). Development of self-healing double-network hydrogels: Enhancement of the strength of wheat gluten hydrogels by in situ metal-catechol coordination. *Journal of Agricultural and Food Chemistry, 67*(23), 6508–6516. https://doi.org/10.1021/acs.jafc.9b01649
Liu, J. M., Li, Q., Zhang, M., Yun, L. Y., & Zhai, J. Y. (2022). Impact of garlic oligosaccharide fractions on microcosmic, mesoscopic, or macroscopic characteristics of dough. *Food Research International, 160*(1), Article 111739. https://doi.org/10.1016/j.foodres.2022.111739
Mao, J., Gao, Y., & Meng, Z. (2023). Crystallization and phase behavior in mixture systems of anhydrous milk fat, palm stearin, and palm oil: Formation of eutectic crystals. *Food Chemistry, 399*(1), Article 133877. https://doi.org/10.1016/j.foodchem.2022.133877
Mao, L., Ma, L., Fu, Y., Chen, H., Dai, H., Zhu, H., … Zhang, Y. (2022). Transglutaminase modified type A gelatin gel: The influence of intra-molecular and inter-molecular cross-linking on structure-properties. *Food Chemistry, 395*(1), Article 133578. https://doi.org/10.1016/j.foodchem.2022.133578
Nhouchi, Z., Botosoa, E. P., Chene, C., & Karoui, R. (2022). Mid infrared as a tool to study the conformational structure of starch and proteins with oil addition during gelatinization. *Lwt-Food Science and Technology, 157*(1), Article 113093. https://doi.org/10.1016/j.lwt.2022.113093
Ni, D., Xu, W., Zhu, Y., Pang, X., Lv, J., & Mu, W. (2021). Insight into the effects and biotechnological production of kestoses, the smallest fructooligosaccharides. *Critical Reviews in Biotechnology, 41*(1), 34–46. https://doi.org/10.1080/07388551.2020.1844622
Qiu, Z., Qiao, Y., Zhang, B., Sun-Waterhouse, D., & Zheng, Z. (2022). Bioactive polysaccharides and oligosaccharides from garlic (Allium sativum L.): Production, physicochemical and biological properties, and structure-function relationships. *Comprehensive Reviews in Food Science and Food Safety, 21*(4), 3033–3095. https://doi.org/10.1111/1541-4337.12972
Renzetti, S., & van der Sman, R. G. M. (2022). Food texture design in sugar reduced cakes: Predicting batters rheology and physical properties of cakes from physicochemical principles. *Food Hydrocolloids, 131*(1), Article 107795. https://doi.org/10.1016/j.foodhyd.2022.107795
Shao, L., Ma, J., Prelesnik, J. L., Zhou, Y., Nguyen, M., Zhao, M., … Chen, C.-L. (2022). Hierarchical materials from high information content macromolecular building blocks: Construction, dynamic interventions, and prediction. *Chemical reviews, 122*(24), 17397–17478. https://doi.org/10.1021/acs.chemrev.2c00220
Sun, Q., Zhang, H., Yang, X., Hou, Q., Zhang, Y., Su, J., … Liu, S. (2023). Insight into muscle quality of white shrimp (Litopenaeus vannamei) frozen with static magnetic-assisted freezing at different intensities. *Food chemistry: X, 17*(1), Article 100518. https://doi.org/10.1016/j.fochx.2022.100518
Sun, X., Wu, S., Koksel, F., Xie, M., & Fang, Y. (2023). Effects of ingredient and processing conditions on the rheological properties of whole wheat flour dough during breadmaking- A review. *Food Hydrocolloids, 135*(1), Article 108123. https://doi.org/10.1016/j.foodhyd.2022.108123
Thanushree, M. P., Sudha, M. L., Martin, A., Vanitha, T., & Kasar, C. (2022). Enhancing the nutritional and quality profiles of buckwheat noodles: Studies on the effects of methods of milling and improvers. *Lwt-Food Science and Technology, 160*(1), Article 113286. https://doi.org/10.1016/j.lwt.2022.113286
Tolstoguzov, V. B. (2000). The importance of glassy biopolymer components in food. *Nahrung-Food, 44*(2), 76–84. https://doi.org/10.1002/(SICI)1521-3803(20000301)44:2<76::AID-FOOD76>3.0.CO;2-D
Vazquez-Vuelvas, O. F., Chavez-Camacho, F. A., Meza-Velazquez, J. A., Mendez-Merino, E., Rios-Licea, M. M., & Carlos Contreras-Esquivel, J. (2020). A comparative FTIR study for supplemented agavin as functional food. *Food Hydrocolloids, 103*(1), Article 105642. https://doi.org/10.1016/j.foodhyd.2020.105642
Wang, B., Huang, B., Yang, B., Ye, L., Zeng, J., Xiong, Z., … Feng, L. (2023). Structural elucidation of a novel polysaccharide from Ophiopogonis Radix and its self-assembly mechanism in aqueous solution. *Food Chemistry, 402*(1), Article 134165. https://doi.org/10.1016/j.foodchem.2022.134165
Wang, P., Wang, G., Zhang, Y., Lv, X., Xie, C., Shen, J., … Jiang, D. (2022). Impact of wheat arabinoxylan with defined substitution patterns on the heat-induced polymerization behavior of gluten. *Journal of Agricultural and Food Chemistry, 70*(46), 14784–14797. https://doi.org/10.1021/acs.jafc.2c05236
Wang, S., Qu, D., Zhao, G., Yang, L., Zhu, L., Song, H., & Liu, H. (2022). Characterization of the structure and properties of the isolating interfacial layer of oil–water emulsions stabilized by soy hull polysaccharide: Effect of pH changes. *Food Chemistry, 370*(1), Article 131029. https://doi.org/10.1016/j.foodchem.2021.131029
Wang, Z., Li, B., Wang, Z., Li, J., Xing, L., Zhou, L., … Yin, H. (2022). Analysis of structural changes and anti-inflammatory capacity in soybean protein isolates conjugated with anthocyanins. *Food Science and Technology, 42*(2), e07922.
Xiao, W., Ding, Y., Cheng, Y., Xu, S., & Lin, L. (2022). Understanding the changes in quality of semi-dried rice noodles during storage at room temperature. *Foods, 11*(14), 2130. https://doi.org/10.3390/foods11142130
Xu, K., Yang, P.-F., Yang, Y.-N., Feng, Z.-M., Jiang, J.-S., & Zhang, P.-C. (2017). Direct assignment of the threo and erythro configurations in polyacetylene glycosides by H-1 NMR spectroscopy. *Organic Letters, 19*(3), 686–689. https://doi.org/10.1021/acs.orglett.6b03855
Yang, X., Pan, Y., Li, S., Li, C., & Li, E. (2022). Effects of amylose and amylopectin molecular structures on rheological, thermal and textural properties of soft cake batters. *Food Hydrocolloids, 133*(1), Article 107980. https://doi.org/10.1016/j.foodhyd.2022.107980
Yazar, G., & Demirkesen, I. (2022). Linear and Non-Linear Rheological Properties of Gluten-Free Dough Systems Probed by Fundamental Methods. *Food Engineering Reviews*, DOI:10.1007/s12393-12022-09321-12393. https://doi.org/10.1007/s12393-022-09321-3.
Zang, Z., Tang, S., Li, Z., Chou, S., Shu, C., Chen, Y., … Li, B. (2022). An updated review on the stability of anthocyanins regarding the interaction with food proteins and polysaccharides. *Comprehensive Reviews in Food Science and Food Safety, 21*(5), 4378–4401. https://doi.org/10.1111/1541-4337.13026
Zhang, N., Jin, M., Wang, K., Zhang, Z., Shah, N. P., & Wei, H. (2022). Functional oligosaccharide fermentation in the gut: Improving intestinal health and its determinant factors-A review. *Carbohydrate Polymers, 284*(1), Article 119043. https://doi.org/10.1016/j.carbpol.2021.119043
Zhou, Y., Dhital, S., Zhao, C., Ye, F., Chen, J., & Zhao, G. (2021). Dietary fiber-gluten protein interaction in wheat flour dough: Analysis, consequences and proposed mechanisms. *Food Hydrocolloids, 111*(1), Article 106203. https://doi.org/10.1016/j.foodhyd.2020.106203